

Spontaneous symmetry breaking in a polariton and photon laser

H. Ohadi,¹ E. Kammann,¹ T.C.H. Liew,² K.G. Lagoudakis,³ A.V. Kavokin,¹ and P.G. Lagoudakis^{1,*}

¹*School of Physics and Astronomy, University of Southampton, Southampton, SO17 1BJ, United Kingdom*

²*Mediterranean Institute of Fundamental Physics, 31, via Appia Nuova, 00040, Rome, Italy*

³*Stanford University, 348 Via Pueblo Mall, Stanford, CA 94305-4088, US*

(Dated: December 2, 2024)

Here we report on the spontaneous formation of polarisation and coherence in an exciton-polariton condensate in a planar GaAs quantum-well microcavity under pulsed excitation. We have measured the Stokes vector of light emitted by the polariton condensate after each excitation pulse. These single-shot measurements evidenced the build-up of stochastic polarisation with the Stokes vector changing randomly from pulse to pulse. Below threshold the polarisation noise does not exceed 10%, while above threshold we observe a total polarisation of about 50% after each excitation pulse, while the polarisation averaged over the ensemble of pulses remains nearly zero. The stochastic polarisation build-up is accompanied by the build-up of spatial coherence of the condensate, evidenced by spatial interferometry measurements. The formation of a stochastic spinor order parameter of the condensate is observed both in strong and weak-coupling regimes, which indicates a striking similarity between polariton and photon lasers.

Bosonic particles cooled below the temperature of quantum degeneracy undergo a thermodynamic phase transition during which phase correlations spontaneously build up and the system enters a macroscopic coherent state. This process is known as Bose-Einstein condensation (BEC). BEC is characterised by a build-up of an order parameter, which is usually associated with a macroscopic multi-particle wave function of the condensate [1]. Recently, observation of BEC of exciton-polaritons in CdTe, GaAs and GaN-based microcavities has been claimed by several groups [2–5]. Several features of BEC have indeed been observed, such as: the macroscopic occupation of a quantum state on top of a Boltzmann-like distribution, the long-range spatial coherence, the spectral narrowing of the photoluminescence signal and the decrease of the second order coherence. While necessary, these signatures are not unambiguous proofs of BEC in exciton-polariton planar microcavities simply due to the fact that these features have also been reported in conventional lasers (Vertical Cavity Surface Emitting Lasers, VCSELs) [6, 7]. One of the characteristic features of this phase transition, spontaneous symmetry breaking has also been proposed as the “smoking gun for BEC” [5]. Polariton lasers show a similar phenomenology to BECs, while from the theoretical point of view there is a significant difference between a polariton BEC and a polariton laser: A polariton BEC, in contrast to a polariton laser, is in thermal equilibrium with the non-condensed polaritons. What terminology should be used for describing degenerate polariton gases is still a subject of debate in the scientific community [8, 9].

Here we report the spontaneous build-up of polarisation and coherence in a GaAs quantum-well microcavity, both in the strong-coupling regime where we observe polariton lasing and, surprisingly, also in the weak coupling where the microcavity is in the photon lasing regime. Our microcavity sample exhibits strong coupling of exciton-

polaritons at low excitation densities, as demonstrated previously [10]. We observe features that can be ascribed both to polariton BEC and polariton lasing in the strong-coupling regime: macroscopic occupation of the ground state on top of a Boltzmann distribution, narrowing of the ground state emission linewidth, long-range spatial coherence, and build-up of stochastic polarisation [11]. Photon lasing was previously reported in the same sample at high excitation densities using a continuous wave source [12]. In pulsed excitation, we observe a dynamical crossover between photon lasing to polariton lasing after a single excitation pulse as the carrier density decreases and the system transfers from weak coupling to strong coupling in agreement with previous observations [13]. We find that both in the strong and weak-coupling regimes the build-up of spatial coherence is correlated with the build-up of stochastic vector polarisation.

The total angular momentum \mathbf{J} of a heavy-hole exciton-polariton in a quantum-well microcavity can have two possible projections on the growth axis of the structure, $J_z = +1$ (spin up) or $J_z = -1$ (spin down), corresponding to right and left circularly polarised emitted light, respectively. The order parameter for an exciton-polariton condensate can then be defined by a two-component complex vector $\psi_\sigma(\mathbf{r}, t) = [\psi_{+1}(\mathbf{r}, t), \psi_{-1}(\mathbf{r}, t)]$, where $\psi_{+1}(\mathbf{r}, t)$ and $\psi_{-1}(\mathbf{r}, t)$ are multi-particle wave functions of the spin-up and spin-down components of the condensate. The components of the complex order parameter ψ_σ are related to the measurable condensate pseudo-spin (Stokes vector) \mathbf{S} by $S_x = \text{Re}(\psi_{-1}^* \psi_{+1})$, $S_y = \text{Im}(\psi_{-1}^* \psi_{+1})$, $S_z = (|\psi_{+1}|^2 - |\psi_{-1}|^2)/2$. The components of the Stokes vector are proportional to the linear, diagonal and circular polarisation degree of light emitted by the condensate. These polarisation degrees define the normalized pseudo-spin vector $\mathbf{s} = 2\mathbf{S}/n$, where n is the occupation number of the con-

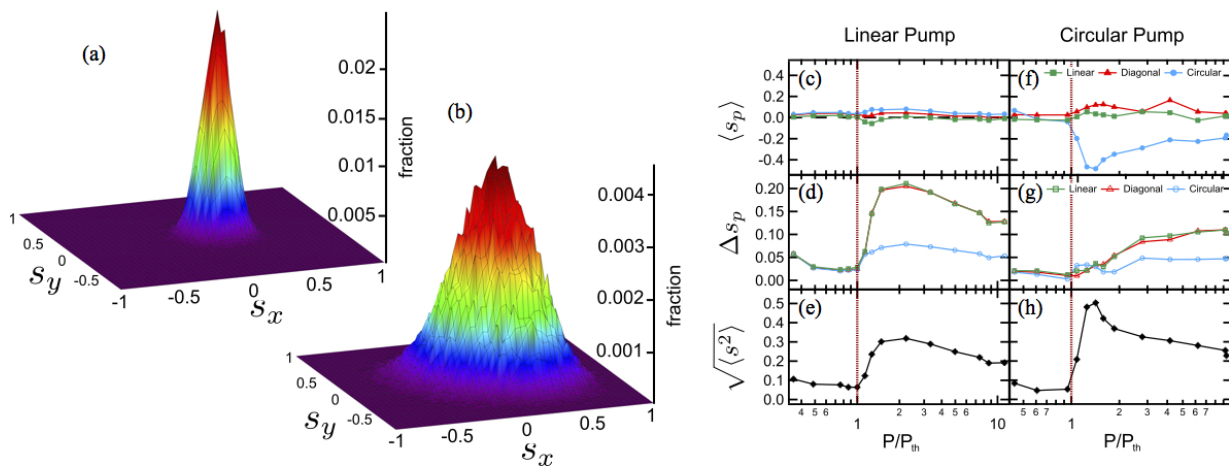


FIG. 1. 2D histogram of linear and diagonal components of the pseudo-spin vector for $P < P_{th}$ (a) and $P = 2.4P_{th}$ (b) on the $x - y$ plane of the Stokes sphere. The mean (c, f), the standard deviation (d, g) and the total degree of polarisation (e, h) for linearly (left panel) and circularly (right panel) polarised pump. Above threshold (marked by a red line) we observe the build-up of total degree of polarisation while the average polarisation remains close to zero for linearly polarised pump.

densate. This vector can be quantified experimentally by polarised photoluminescence (PL) measurements [14, 15]. It contains important information on the order parameter of the condensate. The total degree of polarisation of the emitted light given by the amplitude of \mathbf{s} changes from zero for a chaotic state to 1 for an ideal condensate. The spontaneous symmetry breaking of the condensate manifests itself in the spontaneous build-up of polarisation of the emitted light [16]. In the absence of pinning, this polarisation is randomly chosen by the system and changes stochastically from one experiment to another [17].

The details for the microcavity structure could be found in Ref. [12]. The sample is cooled to ~ 7 K using a cold-finger cryostat. The wedged structure of the microcavity allows accurate probing of the cavity and quantum-well detuning (~ -0.5 meV). The sample is excited non-resonantly into the Bragg mode (~ 0.1 eV above the cavity mode) by 180 fs pulses to make sure that the phase of the excitation laser is lost by multiple relaxations towards the ground state. A high numerical aperture microscope objective (NA = 0.4) focuses the laser ($\lambda = 730$ nm) to a $40 \mu\text{m}$ diameter spot and collects the PL. Imaging the Fourier plane of the emission to a spectrometer allows mapping out of the energy-momentum space. Four fast photomultiplier tubes (PMT) with appropriate polarisers, waveplates and polarising beam-splitters allow simultaneous measurement of the three components of the Stokes parameter for each condensate realisation. A four-channel high sampling rate (5 GS/s, 1 GHz bandwidth, 50 R terminated) digital oscilloscope triggered with the excitation laser records the PMTs photocurrent pulses. The PMTs rise time (~ 1.2 ns) is significantly shorter than the time gap between sequential pulses at the repetition rate of the laser ($f_{rep} = 76$ MHz) allowing individual resolution of the PL pulses. Extra

care is taken to accurately calibrate the PMTs and waveplates. To eliminate any artefacts from the polarisation optics we place a polarizer immediately after the microscope objective followed by individually calibrated half and quarter waveplates to adjust the PMTs relative gains to their corresponding polarisation basis. About 64,000 shots are recorded and analysed for different polarisations and powers of the excitation laser. The components of the normalized pseudo-spin vector \mathbf{s} are measured by $s_{x,y,z} = (I_{0^\circ,45^\circ,\circ} - I_{90^\circ,-45^\circ,\circ}) / (I_{0^\circ,45^\circ,\circ} + I_{90^\circ,-45^\circ,\circ})$, where I is the peak intensity of the PL pulse recorded by the PMT to an accuracy of $> 94\%$. Polarisation distributions were deconvoluted with the intrinsic noise of the detection system. The PL can be spectrally filtered by means of a grating and an adjustable slit before focusing into the PMTs.

Here we measure and record the polarisation of emitted light after each excitation pulse. This measurement is integrated over the lifetime of each individual condensate excited by a laser pulse. On the other hand, we do not average on the ensemble of pulses, but we perform single-shot polarisation measurements. Figure 1a,b shows the 2D projection of the Stokes parameter histogram on the $x - y$ plane (linear polarisation plane) for 64,000 shots. In the linear regime and when the pump power is below threshold (Fig. 1a) we observe a narrow Gaussian distribution centred to zero, which demonstrate the unpolarised nature of the polariton PL. The width of the Gaussian distribution is limited by the analogue noise and the finite digital sampling rate of the acquisition. Above threshold ($P = 2.4P_{th}$) and still in the strong-coupling regime (Fig. 1b) the distribution significantly broadens, with the average polarisation again remaining close to zero. Although the average polarisation in the strong-coupling regime is zero we see that each realisa-

tion of the condensate is indeed polarised with a random orientation of the Stokes vector.

Fig. 1c-h shows the mean degree of polarisation, the standard deviation (Δs) and average degree of polarisation for linear and circular pump polarisation. The increase of standard deviation of polarisation in the ensemble of shots is a manifestation of the stochastic build-up of polarisation. Contrary to other microcavity samples [18, 19] we do not observe any polarisation pinning to the crystallographic axes and below threshold the polarisation is unpolarised for linear pumping. The total degree of polarisation increases above threshold followed by a sharp drop with increasing pump power.

In the strong-coupling regime the density of electron-hole pairs remains below the Mott transition, where the Coulomb attraction is sufficient to stabilise Wannier-Mott excitons. By increasing the excitation beyond the Mott transition density the excitons ionize and an electron-hole plasma is formed [20, 21]. Energy-resolved Fourier space imaging allows for direct evidence of both the strong and the weak-coupling regime as the corresponding dispersion relations ($E(k)$) are fundamentally different. Above threshold and still in the strong-coupling regime ($P = 1.1P_{th}$) we observe a blue-shifted lower exciton-polariton emission and as we increase the power ($P > 4P_{th}$) we enter the weak-coupling regime and an emission peak near the bare cavity photon energy emerges [11].

Using a grating and a variable mechanical slit we can spectrally filter the photoluminescence emission of polaritons (strong coupling) or bare cavity photon energy (weak coupling). Fig. 2a, b and c show the dispersion for the linear, strong-coupling and weak-coupling regime respectively. The cyan border displays the energy gap that is filtered for the measurement. Fig. 2d shows the total degree of polarisation of photon and polariton energy states for linearly and circularly polarised pump. The observed total degree of polarisation at bare cavity photon energy is twice higher than that of the polariton states.

A theoretical description of the stochastic polarisation build-up in the strong coupling regime can be based on the development of the Langevin equation for exciton-polaritons [17], which replaces the Fokker-Planck equation for distribution functions with a stochastic element. Within this theory, which is described in detail in the Supplementary Information, each pulse in the experiment is modelled separately and receives an influx of polaritons with random polarisation from the hot incoherent excitons excited by the non-resonant pump. Below threshold, the polariton polarisation changes rapidly within the duration of each pulse since polaritons excited in the system have uncorrelated stochastic polarisation. Equivalently, there is no coherence between polaritons and the total polarisation degree (whether averaged over multiple pulses or not) is minimal.

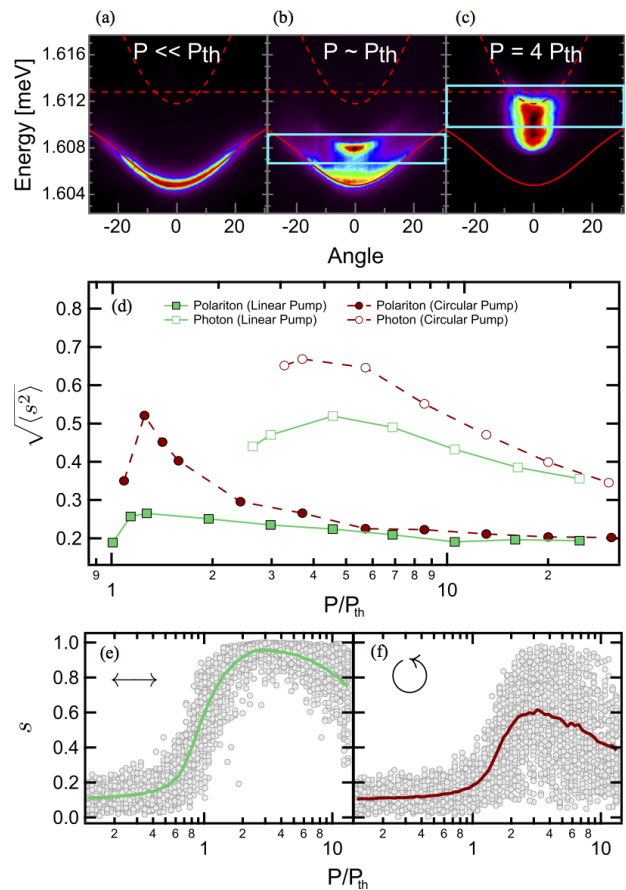


FIG. 2. Dispersion images for (a) below threshold (linear regime), (b) $P = 1.5P_{th}$ (strong-coupling regime) and (c) $P = 4P_{th}$ (weak-coupling regime). The cyan border marks the regions that are filtered for polariton states (b) and bare cavity photon states (c). (d) The total degree of polarisation for circularly polarised (dotted lines) and linearly polarised pump (solid lines) for photon (open circles) and polariton energy states (closed circles). (e), (f) Simulation results for the dependence of the total polarisation degree on pump intensity for a linearly polarised (e) and circularly polarised (f) pump. The grey circles show the values for each pulse and the solid curves show the pulse-averaged values.

Above threshold, stimulated scattering amplifies the polarisation state of polaritons. Polaritons become coherent and a high total polarisation degree is expected in each pulse. In the absence of pinning, this polarisation is randomly chosen by the system and changes stochastically from one pulse to another. This effect appears both experimentally (Fig. 2d) and theoretically (see Fig. 2f), however, our theory predicts larger polarisation degrees than those observed experimentally. This is to be expected since the theory does not take into account the spatial inhomogeneity of the condensate.

It is important to note that since the average linear polarisation degrees observed in our system are minimal (Fig. 1c), we expect that only a small polarisation splitting is present in the sample. For this reason there is

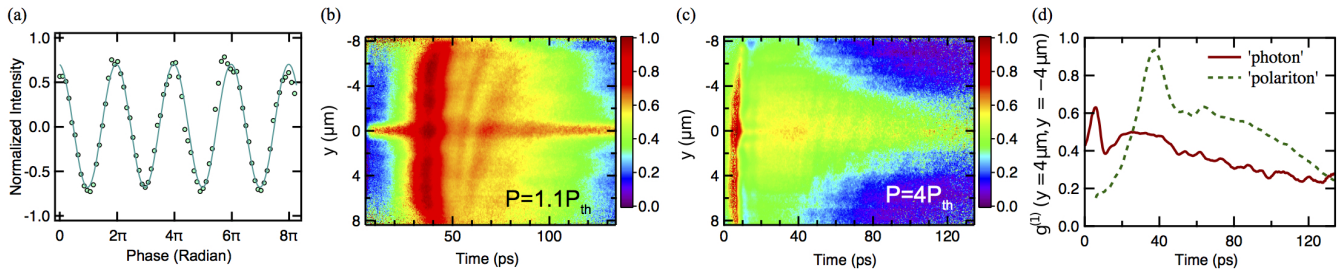


FIG. 3. (a) Normalized intensity on one pixel as a function of phase between the arms of the interferometer. The first-order coherence $g^{(1)}(\mathbf{r}, -\mathbf{r})$ is given by the amplitude. Time resolved first-order spatial coherence, taken across the autocorrelation point at (b) $P = 1.1P_{th}$ and (c) $P = 4P_{th}$. (d) The first-order coherence as a function of time in polariton and photon laser regimes.

minimal spin relaxation or rotation of the Stokes vector, at moderate densities, after the polarised polariton condensate has formed in each pulse. However, for high polariton densities the anisotropy of polariton-polariton interactions introduces a nonlinear mechanism of Stokes vector precession known as self-induced Larmor precession [22]. This mechanism causes the reduction of the total polarisation degree, which is time integrated over the duration of each pulse, for increasing pump intensity in both experiment and theory.

Under circularly polarised pumping the presence of a non-zero circular polarisation degree of the polariton condensate demonstrates incomplete spin relaxation of the excited carriers in our experiment (Fig. 1f). Theoretically, this is accounted for by a partial spin relaxation between hot exciton reservoirs. Note that the incomplete spin relaxation does not imply that any phase coherence is preserved from the non-resonant laser.

To reveal the build-up of coherence, the first-order spatial correlation function ($g^{(1)}(\mathbf{r}, -\mathbf{r})$) of the polariton emission is studied using an actively-stabilised Michelson interferometer in a mirror-retro-reflector configuration (for details see Ref. [2]). To time-resolve the correlation function a diffraction-limited 1-dimensional stripe of the interferograms is sent to a streak camera [23]. By scanning the phase between the mirror and the retro-reflector arm (Fig. 3a) $g^{(1)}(\mathbf{r}, -\mathbf{r})$ can be extracted. Time-resolved real-space correlation functions are shown in Fig. 3b and Fig. 3c for $P = 1.5P_{th}$ and $P = 4P_{th}$ respectively. Fig. 3b shows the macroscopic phase coherence for the exciton-polariton condensate. In Fig. 3c we observe a high degree of coherence for photon lasing along the whole real space profile. In the transition to polariton lasing the coherence drops significantly and builds up again when the system enters the strong-coupling (Fig. 3d), but with a lower degree of coherence due to the lower occupation of the ground state [11].

In conclusion our work has provided an experimental evidence of the spontaneous symmetry breaking in the exciton-polariton lasing regime where the polarisation of emission is not pinned to the crystal geometry or struc-

tural defects. Interestingly we have also observed spontaneous symmetry breaking in the photon lasing regime where the system is weakly coupled. We have observed formation of stochastic, randomly oriented, vector polarisation of the condensate combined with the build-up of macroscopic coherence. Our experimental results are in agreement with the theoretical model in the exciton-polariton regime.

P.G.L. and A.V.K. would like to acknowledge the FP7 ITN-Spinoptronics, ITN-Clermont 4, Royal Society and EPSRC through contract EP/F026455/1 for funding. The authors thank Jacqueline Bloch and Aristide Lemaître for provision of the sample.

* correspondence address: pavlos.lagoudakis@soton.ac.uk

- [1] O. Penrose and L. Onsager, *Physical Review* **104**, 576 (1956).
- [2] J. Kasprzak *et al.*, *Nature* **443**, 409–14 (2006).
- [3] R. Balili *et al.*, *Science* **316**, 1007 (2007).
- [4] H. Deng *et al.*, *Science* **298**, 199 (2002).
- [5] J. Baumberg *et al.*, *Phys. Rev. Lett.* **101**, 136409 (2008).
- [6] M. van Exter *et al.*, *IEEE J. Sel. Top. Quantum Electron.* **1**, 601 (1995).
- [7] R. Jin *et al.*, *J. Nonlinear Opt. Phys. Mater.* **4**, 141 (1995).
- [8] L. V. Butov and A. V. Kavokin, *Nat. Photon.* **6**, 2 (2012).
- [9] B. Deveaud-Plédran, *J. Opt. Soc. Am. B* **29**, A138 (2012).
- [10] M. Maragkou *et al.*, *App. Phys. Lett.* **97**, 111110 (2010).
- [11] E. Kammann *et al.*, [arXiv:1103.4831](https://arxiv.org/abs/1103.4831) (2011).
- [12] D. Bajoni *et al.*, *Phys. Rev. B* **76**, 201305 (2007).
- [13] B. Nelsen *et al.*, *J. App. Phys.* **105**, 122414 (2009).
- [14] P. G. Lagoudakis *et al.*, *Phys. Rev. B* **65**, 161310 (2002).
- [15] A. Kavokin *et al.*, *Phys. Rev. B* **67**, 195321 (2003).
- [16] F. P. Laussy *et al.*, *Phys. Rev. B* **73**, 035315 (2006).
- [17] D. Read *et al.*, *Phys. Rev. B* **80**, 195309 (2009).
- [18] J. Kasprzak *et al.*, *Phys. Rev. B* **75**, 045326 (2007).
- [19] G. Christmann *et al.*, *App. Phys. Lett.* **93**, 051102 (2008).
- [20] L. Kappei *et al.*, *Phys. Rev. Lett.* **94**, 147403 (2005).
- [21] M. Stern *et al.*, *Phys. Rev. Lett.* **100**, 256402 (2008).
- [22] I. Shelykh *et al.*, *Phys. Rev. B* **70**, 035320 (2004).
- [23] G. Nardin *et al.*, *Phys. Rev. Lett.* **103**, 256402 (2009).